THE BELL SYSTEM TECHNICAL JOURNAL

DEVOTED TO THE SCIENTIFIC AND ENGINEERING ASPECTS OF ELECTRICAL COMMUNICATION

Volume 60 May–June 1981 Number 5

Dispersionless Single-Mode Lightguides With α Index Profiles

By U. C. PAEK, G. E. PETERSON, and A. CARNEVALE

(Manuscript received November 14, 1980)

By means of a numerical solution to Maxwell's equations, we calculate those parameters necessary to design and fabricate single-mode lightguides. These include optimum core radius and profile parameter α. In the design the dispersion is minimized by varying the core radius while the relative index difference Δ, the wavelength λ, and profile parameter are held fixed. A comparison of calculated dispersion with experimental data shows excellent agreement.

I. INTRODUCTION

Recently, single-mode lightguides have been developed that achieve transmission losses as low as 0.5 dB/km and 0.2 dB/km at wavelengths of 1.3 μm and 1.55 μm, respectively.[1] When the total lightguide dispersion is reduced to zero at the operating wavelength, a transmission system can be realized with wide repeater spacings and extremely large bandwidths.[2-4] In fact, bandwidths in excess of 1 GHz/100 km are expected. Clearly, such a lightguide system would be ideal for undersea cable and other long-distance transmission applications.

The design of single-mode lightguides with zero total dispersion requires an accurate description of this parameter in terms of profile shape, materials properties, and core radius. This necessitates a solution of Maxwell's equations for the fundamental HE_{11} lightguide mode as well as the TE_{01} and TM_{01} modes.

For radially inhomogeneous media, it is usually not possible to obtain these solutions as analytical expressions of a closed form. To a

very large extent the design of single-mode lightguides has in the past focused on rectangular-shaped index profiles. This is because Maxwell's equations are very much easier to solve in this case. When nonrectangular profiles have been considered, numerous approximations have often been employed.

To avoid these difficulties, we have developed a numerical technique to obtain exact solutions to the vector form of Maxwell's equations.[5] These equations are written as four coupled simultaneous first-order differential equations. The effective index N_e for the single propagating HE_{11} mode is found by solving the characteristic equation derived from the matching conditions of the field components at the core cladding interface. The dispersion is then calculated from N_e. In addition, we find the conditions under which the TE_{01} and TM_{01} modes propagate.

Our computing procedures do not impose any restrictions on the index profile of the fiber.[5,6] However, for the sake of simplicity and familiarity we choose the α-index profile. To confirm the analysis, we compare the computed results with known experiments when possible. The calculated results include the dispersion, the optimum core radius (defined as the value at which the zero total dispersion will occur for a given relative index difference, wavelength, and α value), and the corresponding cutoff frequency.

To keep the accuracy as high as possible, material dispersion is included in the calculation from the onset. The subtle interaction between material properties and waveguide properties determine the propagation characteristics of the lightguide. Details of the numerical procedure can be found in the appendix.

II. DESIGN OF A DISPERSIONLESS SINGLE-MODE FIBER

In the design of a single-mode fiber, the relative index difference Δ, the operating wavelength λ, and the cladding index N_2 are normally specified. The objective of the design is to make the total dispersion for the HE_{11} mode equal to zero, the total dispersion D_t being defined as the time spread of a narrow pulse per fiber length L per source spectral width $d\lambda$. Qualitatively speaking, this can be accomplished by adjusting the radius and profile shape so that the waveguide dispersion exactly counterbalances the material dispersion. In addition, the design must be such that the TE, TM, and other higher-order HE and EH modes are not propagating. In the analysis shown in the appendix, the number of modes allowed to propagate in the fibert core are not restricted. However, the single-mode analysis is nothing but a particular case of multimode propagation and it can be easily achieved simply by setting the angular mode number $M = 0$ and 1 in the elements of matrix A [eq. (18) in the appendix] while fixing the radial

mode number $Q = 1$. When $M = 0$, the cutoff frequency for the TE_{01} and TM_{01} can be determined. Below this cutoff point, only a fundamental mode (HE_{11}) propagate in the fiber. All the modes other than $M = 0$ are hybrid modes. Further details are explained below.

When eqs. (22) and (23) are substituted into eq. (21), determinant (21) decomposes into two uncoupled equations, giving the *TM* and *TE* modes,

TM mode:

$$\frac{(\beta_1^2\Lambda_{21} - \kappa(\zeta_i)\gamma_0\Lambda_{11})}{(\beta_1^2\Lambda_{22} - \kappa(\zeta_i)\gamma_0\Lambda_{12})} = 1. \tag{1}$$

TE mode:

$$\frac{(\beta_1^2\Lambda_{32} - \gamma_0\Lambda_{42})}{(\beta_1^2\Lambda_{31} - \gamma_0\Lambda_{41})} = 1. \tag{2}$$

When N_1 is the maximum value of the index of refraction in the core and N_2 is the cladding index, the effective index of the bounded modes must satisfy the condition $N_2 < N_e < N_1$. Therefore, from eqs. (1) and (2) the effective index $N_e(0, 1)$ for the TM_{01} and TE_{01} mode can be found.[5] The notation $N_e(M, Q)$ refers to the effective index of a mode having angular mode number M and radial mode number Q.

In practice, the core radius is changed until $N_e(0, 1)$ is equal to N_2. This gives us the cutoff radius a_c. for the TE_{01} and TM_{01} modes. The normalized cutoff frequency is then calculated from

$$V_C = \frac{2\pi a_c}{\lambda}\sqrt{N_1^2 - N_2^2}. \tag{3}$$

Now if $V < V_c$, only a single mode (HE_{11}) propagates. The effective index N_e for this mode is calculated in the single-mode region as a function of the radius and is the principal quantity used to determine the dispersion of the HE_{11} mode.

The relationship between the effective index $N_e(1, 1)$ and the group index N_g is given by

$$N_g = N_e - \lambda\frac{dN_e}{d\lambda}. \tag{4}$$

The propagation time of a pulse through a fiber of length L and group index N_g is

$$t = \frac{L}{C}N_g. \tag{5}$$

If there is a variation of N_g with wavelength, there is a dispersion or spread in pulse width. Thus

$$dt \cong \frac{L}{C}\frac{dN_g}{d\lambda}d\lambda, \tag{6}$$

where $d\lambda$ is the spectral width of the source.

We can substitute N_g from eq. (4) into eq. (6) and get

$$dt = -\frac{L}{C}(d\lambda)\lambda\frac{d^2N_e}{d\lambda^2}. \tag{7}$$

The total dispersion D_t is

$$D_t = \frac{dt}{d\lambda}\cdot\frac{1}{L}. \tag{8}$$

Thus,

$$D_t = -\frac{\lambda}{C}\frac{d^2N_e}{d\lambda^2}. \tag{9}$$

Obviously, we need to solve Maxwell's equations for N_e and then calculate $d^2N_e/d\lambda^2$ to obtain D_t.

Following the procedure described in our earlier papers, it is convenient to describe the dispersive properties of the cladding by a modified Sellmeier formula.[5,7] Thus,

$$N_2 = C_0 + C_1\lambda^2 + C_2\lambda^4 + \frac{C_3}{(\lambda^2 - l)} + \frac{C_4}{(\lambda^2 - l)^2} + \frac{C_5}{(\lambda^2 - l)^3}, \tag{10}$$

where $l = 0.035$. The coefficients C_i are given in Table I. Figure 1 shows the variation of the silica cladding's refractive index, for the lightguides considered here.

Since the relative index difference Δ is rather small, typically ranging from 0.2 percent to 0.8 percent, the core center index N_1 can be written as

$$N_1 = \frac{N_2}{[1 - \Delta]}. \tag{11}$$

To obtain a feel for the size of the numbers involved, the following data are useful:

$$\lambda = 1.33\ \mu\text{m},$$

$$N_2 = 1.446925,$$

$$N_1 = 1.449825\ \text{[as calculated by eq. (11)]}.$$

Table I

C_0 =	1.4508554
C_1 =	−0.0031268
C_2 =	−0.0000381
C_3 =	0.0030270
C_4 =	−0.0000779
C_5 =	0.0000018

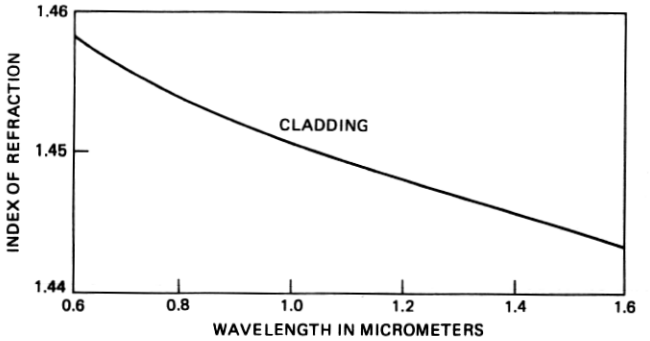

Fig. 1—Refractive index of silica as a function of wavelength.

Since we assume a wavelength dependence for N_2, described by eq. (10), N_1 as calculated by eq. (11) is also wavelength dependent. The following profile formula is particularly useful and will be employed in the fiber design:

$$N(r) = N_1[1 - \Delta r^{\alpha}]. \tag{12}$$

A few comments seem in order: When $\alpha \to \infty$ the profile is rectangular, when $\alpha = 2$ it is parabolic, when $\alpha = 1$ it becomes linear, and when $\alpha < 1$ the profile develops a cusp. Figure 2 illustrates these shapes.

In practice, one specifies Δ, λ, and the profile parameter α. The computer then searches for a core radius that makes $D_t = 0$ by means of Mueller's iterative method. If it can be assumed that the total dispersion is the sum of waveguide dispersion $D_w(\lambda, a, \alpha, \Delta)$ and material dispersion $D_m(\lambda)$, then the physics of the problem is easy to understand. As will be shown later, this separation is quite accurate. Thus, a dispersionless single-mode fiber is one in which material dispersion is exactly balanced by waveguide dispersion. This is illustrated by Fig. 3.

Curve $D_m(\lambda)$ shows the material dispersion as a function of wavelength for a single-mode lightguide with $\Delta = 0.2$ percent and a rectangular profile. Note that it changes sign and passes through zero at about 1.27 μm. Also plotted are waveguide dispersion curves for three different radius values. Note that all three curves are negative and that as the radius *decreases* the magnitude of the dispersion increases at a given wavelength.

From Fig. 3 we can draw a number of conclusions. First, the lightguide with the materials properties shown can be made totally dispersion free only at wavelengths longer than 1.27 μm. Second, as the wavelength gets longer the guide radius must get smaller. Finally, at longer wavelengths a much larger amount of material dispersion

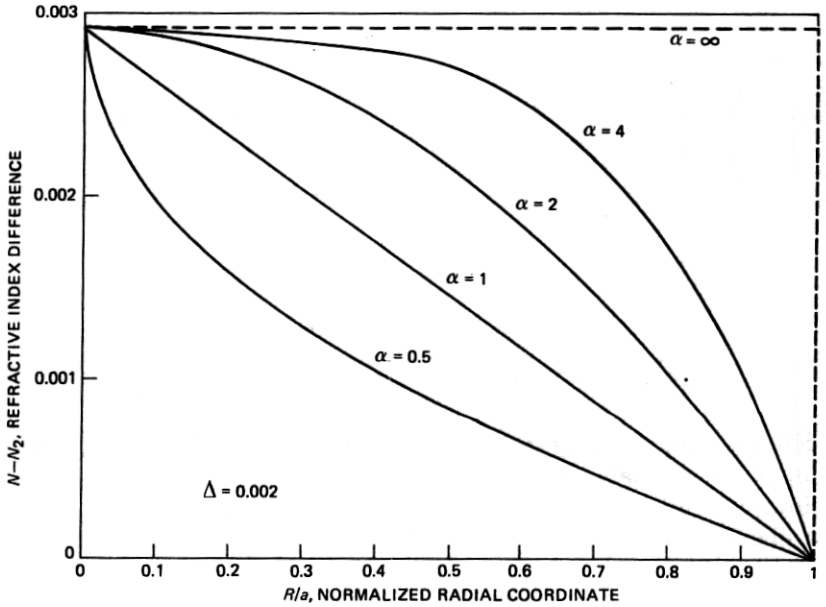

Fig. 2—Index profile shapes for various power laws. When $\alpha \rightarrow \infty$ the profile is rectangular, when $\alpha = 2$ it is parabolic, and when $\alpha = 1$ it is linear. If α is less than 1, the profile develops a cusp.

must be compensated for by waveguide dispersion. This requires greater precision in the waveguide parameters than when the guide is designed to operate at the zero of material dispersion. Hence, it is desirable to have a variety of materials available for lightguide design purposes.

Finally, a typical total dispersion curve D_t, illustrating lightguide operation at 1.3 μm, is plotted in Fig. 3.

III. SINGLE-MODE LIGHTGUIDES WITH α PROFILES FOR 1.33-μm OPERATION

Single-mode lightguides that are designed to operate at 1.33 μm with $\Delta = 0.2$ percent are of much current interest. The cutoff frequencies $V_c(\alpha)$ for the α-index profiles can be found from eqs. (1) and (2). Figure 4 plots the results. There is little change in V_c until the profile parameter is below 10, then it increases rapidly. At $\alpha = 1$, V_c and V_{opt} are 4.383 and 2.724, respectively. The data of Fig. 4 agree well with that in the literature.[8,9]

To determine the radius a_{opt} for zero total dispersion, a computer search is done for values less than a_c, where a_c is the cutoff radius [see eq. (3)]. Figure 5 shows the result for three α values, namely 100, 2, and 1. The radii turn out to be 4.142, 5.725, and 6.294, respectively.

Note that the total dispersion D_t is most sensitive to the radius for $\alpha = 100$, and least sensitive when $\alpha = 1$. For design purposes, we plot a_{opt} as a function of the profile parameter α in Fig. 6. This plot also includes the cutoff wavelength λ_c, where λ_c is defined by the following formula:

$$\lambda_c = (V_{opt}/V_c) \cdot \lambda. \tag{13}$$

Note that both V_{opt} and V_c are employed in the calculation. Therefore, to allow only one mode to propagate in the core, the operating wavelength must be longer than the cutoff wavelength λ_c. For a step index profile with $\Delta = 0.2$ percent and $\lambda = 1.33$ μm, λ_c is close to 1 μm.

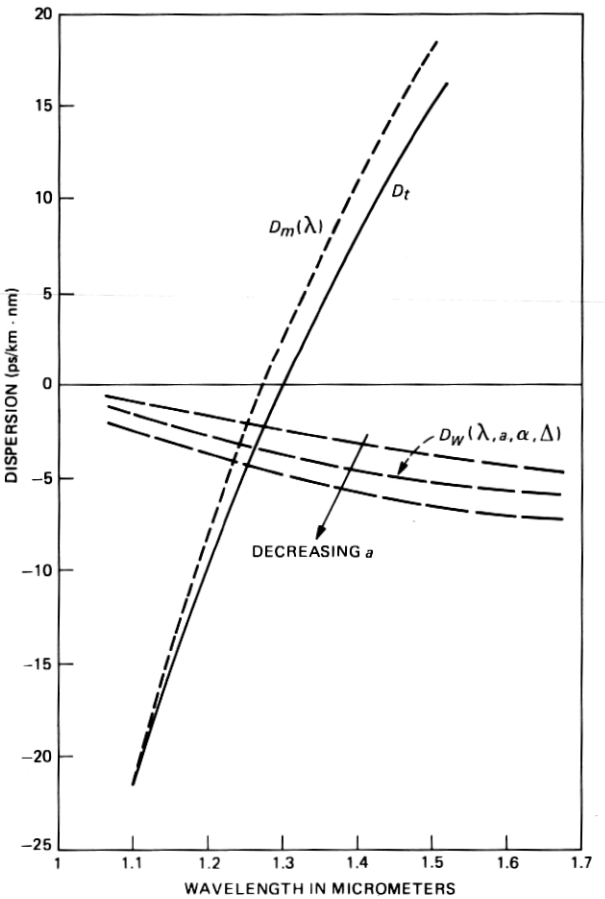

Fig. 3—A plot showing material dispersion D_m, waveguide dispersion D_w, and total dispersion D_t. Note that because of the difference in sign between the material dispersion and the waveguide dispersion it is possible for one to cancel the other at a particular wavelength.

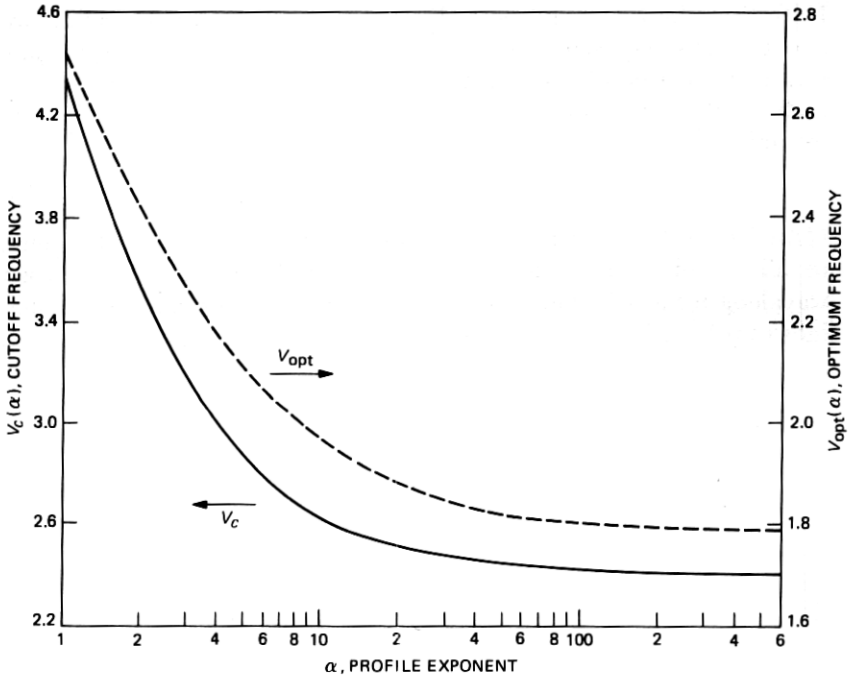

Fig. 4—A plot of V_c and V_{opt} as a function of the profile parameter.

The calculations described thus far in this section have made no assumption concerning the separation of the total dispersion D_t into its component parts D_m and D_w. Our numerical procedure simply searches for a zero in total dispersion and does not assume that $D_t = D_m + D_w$.

However, the material dispersion contribution can be calculated directly by means of eqs. (10) and (9), where N_2 is substituted for N_e. The waveguide dispersion can be found by solving Maxwell's equations numerically via the procedure outlined in the appendix, with N_2 being wavelength independent.

Figures 7a through 7c show the results for $\alpha = 100$, 2, and 1. In all three figures the material dispersion, which is of course independent of core radius, is represented by the horizontal dashed line. The negatives of the waveguide dispersions are dependent on core radius and are the solid lines in the figures. The intersection of the solid and dashed lines yields the optimum radii. As is evident from the figures, the radii are identical with the previous calculations.

IV. A COMPARISON WITH EXPERIMENTAL DATA

Miya, Terunuma, and Hosaka[10] have fabricated GeO_2 doped single-

mode lightguides for the 1.3 μm and 1.5 μm region. Their experimental data are very useful to check the theory presented in this paper. They give data on a fiber with $\Delta = 0.2$ percent and a zero total dispersion at $\lambda = 1.33$ μm. A second fiber has $\Delta = 0.74$ percent and a zero total dispersion at $\lambda = 1.54$ μm. Both are step-index fibers. Their experimental data are measured with a fiber Raman laser excited by a Q switched, mode-locked Nd:YAG laser. The spectral range studied is 1.1 to 1.7 μm. The optimum radius is 4.142 μm for $\Delta = 0.2$ percent and

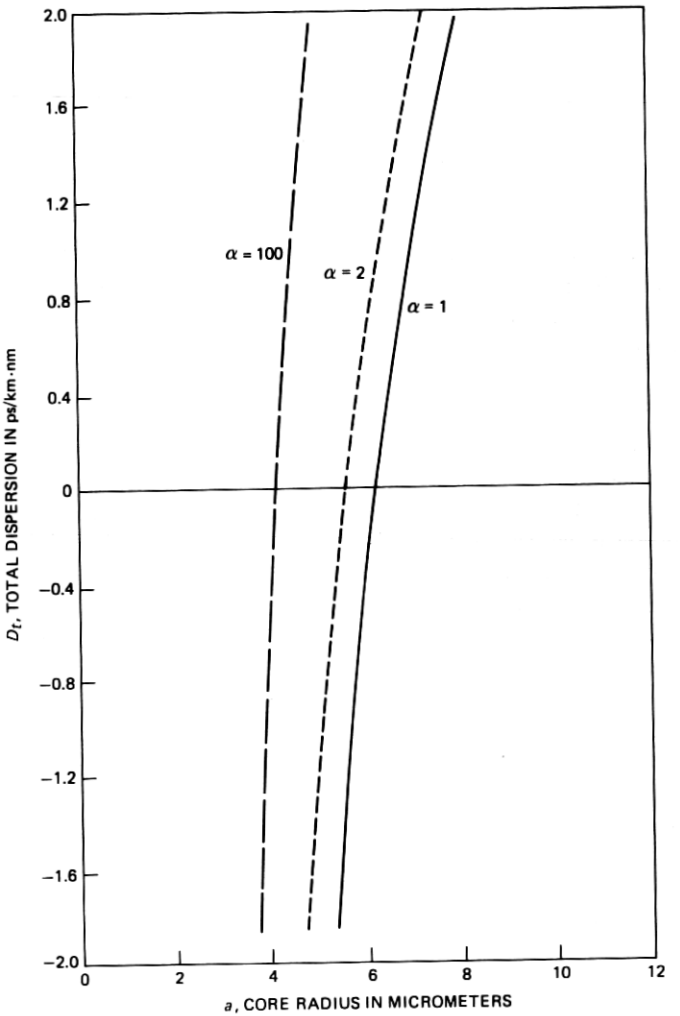

Fig. 5—Total dispersion versus core radius for lightguides with $\alpha = 1$, $\alpha = 2$, and $\alpha = 100$. Note that the total dispersion curve is steepest for $\alpha = 100$ and shallowest for $\alpha = 1$.

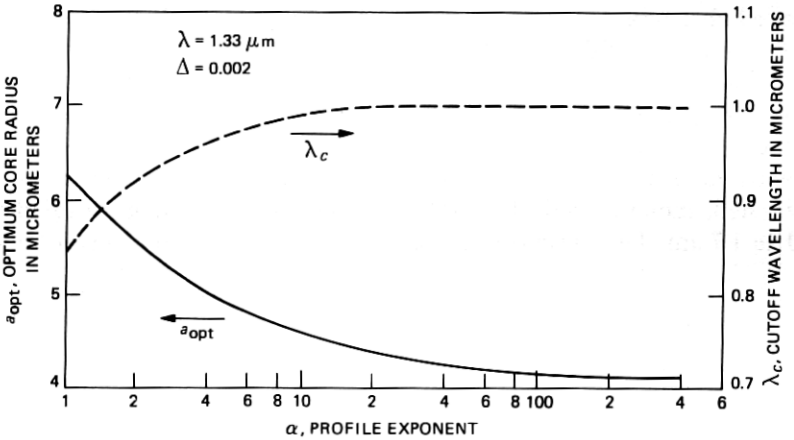

Fig. 6—A plot of cutoff wavelength λ_c and optimum radius a_{opt} versus α. This data is very useful for design purposes.

$\lambda = 1.33$ μm. The optimum radius is 2.30 μm for $\Delta = 0.75$ percent and $\lambda = 1.53$ μm. Figure 8 compares their experimental results (circles and triangles) with our calculations (solid and dashed lines). The agreement is excellent.

V. DISCUSSION

At a wavelength of 1.33 μm, dispersion-free lightguides can be designed with improved properties over the rectangular profile guides. Our calculated results of a_{opt} and cutoff frequency $V_c(\alpha)$ both show a rapid increase as the profile parameter α drops below 10. For a triangular index profile ($\alpha = 1$), the core size is over 50 percent larger than the size of a step-index core. Thus, due to ease of handling, coupling to the source, and splicing, a larger core size is desirable for the same value of Δ and λ.

As the profile parameter α drops below 10, V_{opt} also begins to increase substantially. It is significant that in the case of $\alpha = 1$, $V_{opt} \sim 2.7$, which is a substantial increase over the step-index case, $V_{opt} \sim 1.8$.[11,12]

In addition, Fig. 5 shows that a lightguide with a triangular profile is less susceptible to variations in core radius than a step-index guide. Therefore, because of the larger core size and less sensitivity in its tolerance, a triangular profile may be less difficult to fabricate than a rectangular profile.

VI. ACKNOWLEDGMENTS

We wish to thank M. I. Cohen, R. J. Klaiber, and L. S. Watkins for their helpful discussions and encouragements.

APPENDIX

To study the propagating modes in a fiber, we first assume that the cross section of the fiber is concentric in the core and cladding and that the core diameter $2a$ is much smaller than the outer diameter D (Fig. 9). Further, we assume that the core is a lossless, radially inhomogeneous medium with a scalar permittivity ϵ. A relative permittivity (dielectric constant) is defined by $\kappa = \epsilon/\epsilon_0$, where ϵ_0 is the value in free space. However, as is well known in a nonconducting medium, the permittivity becomes equal to the square of the index of refraction N. For source-free fields in a dielectric waveguide, Maxwell's equations reduce to

$$\nabla \times E = -\mu_0 \frac{\partial H}{\partial t}, \qquad \nabla \times H = \epsilon_0 \kappa \frac{\partial E}{\partial t}, \tag{14}$$

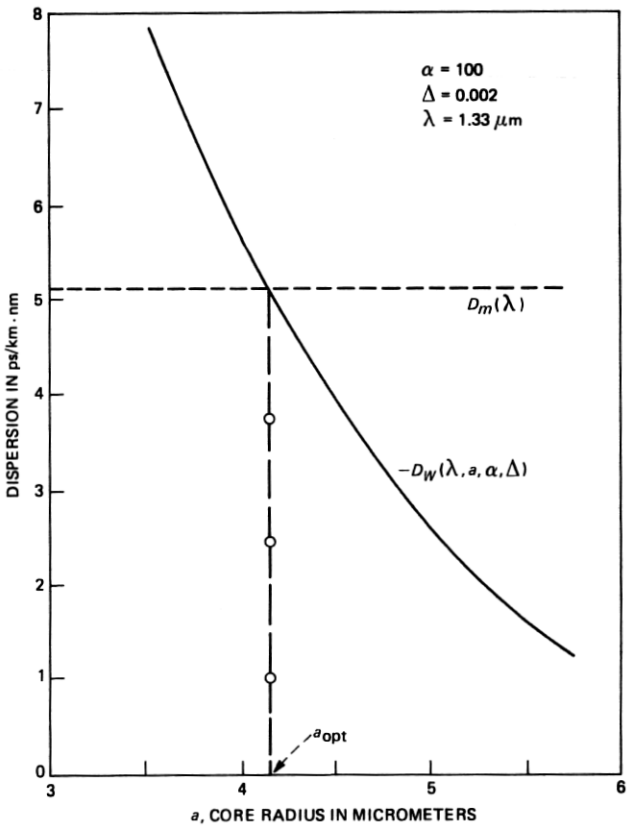

Fig. 7(a)—A plot of waveguide dispersion and material dispersion as a function of core radius, $\alpha = 100$.

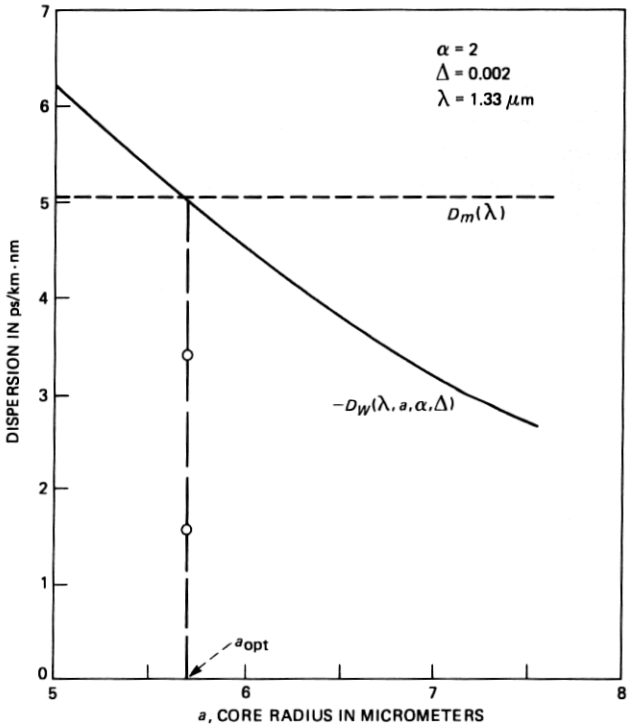

Fig. 7(b)—A plot of waveguide dispersion and material dispersion as a function of core radius, $\alpha = 2$.

where $E(\mathbf{R}, t)$ and $H(\mathbf{R}, t)$ represent the electric and magnetic fields. μ_0 is a scalar permeability in free space.

In a cylindrical coordinate system $\mathbf{R} = \{R, \phi, z\}$, the solution of eq. (14) is described by the vector components of two fields, $\{E_R, E_\phi, E_z\}$ and $\{H_R, H_\phi, H_z\}$. Among these components we are primarily interested in finding the tangential components $\{E_\phi, E_z\}$ and $\{H_\phi, H_z\}$. These will be continuous through the core-cladding interface. Once the tangential components are known, the radial components E_R and H_R can be obtained from these components. To find a complete set of bounded modes we consider the following form of solution:[13]

$$E(\rho, \phi, z, t) = E(\rho) \exp[i(\omega t - M\phi - \beta z)], \tag{15}$$

where ω and M are angular frequency and mode number, and β is propagation constant along the z axis.

Introducing a new variable Λ, the field components are written as

$$\Lambda = \begin{Bmatrix} \Lambda_1 \\ \Lambda_2 \\ \Lambda_3 \\ \Lambda_4 \end{Bmatrix} = \begin{Bmatrix} E_z \\ -iZ_0\rho H_\phi \\ \rho E_\phi \\ -iZ_0 H_z \end{Bmatrix}, \tag{16}$$

where $\rho = KR = 2\pi R/\lambda$, Z_0 is the wave impedance defined by (μ_0/ϵ_0),[1,2] and λ is a wavelength.

Substituting eq. (16) into eq. (15) yields a set of the first-order ordinary differential equations.[13,14] In the following equation,

$$\frac{d\Lambda}{d\rho} = \frac{1}{\rho} A(\rho)\Lambda, \tag{17}$$

the operator $A(\rho)$ is a 4×4 matrix that contains important property constants and parameters, for instance, the index of refraction N, angular mode number M, and the effective index N_e defined by β/k.

The 4×4 matrix $A(\rho)$ can be written as

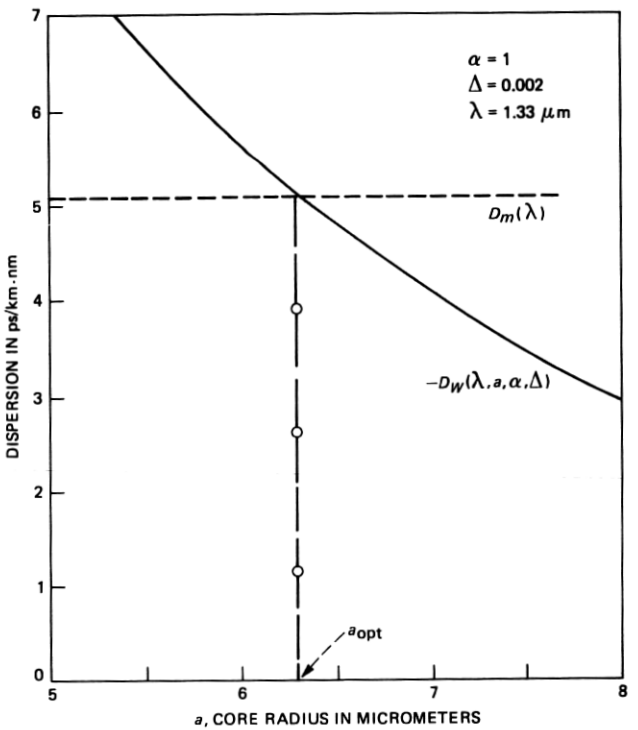

Fig. 7(c)—A plot of waveguide dispersion and material dispersion as a function of core radius, $\alpha = 1$.

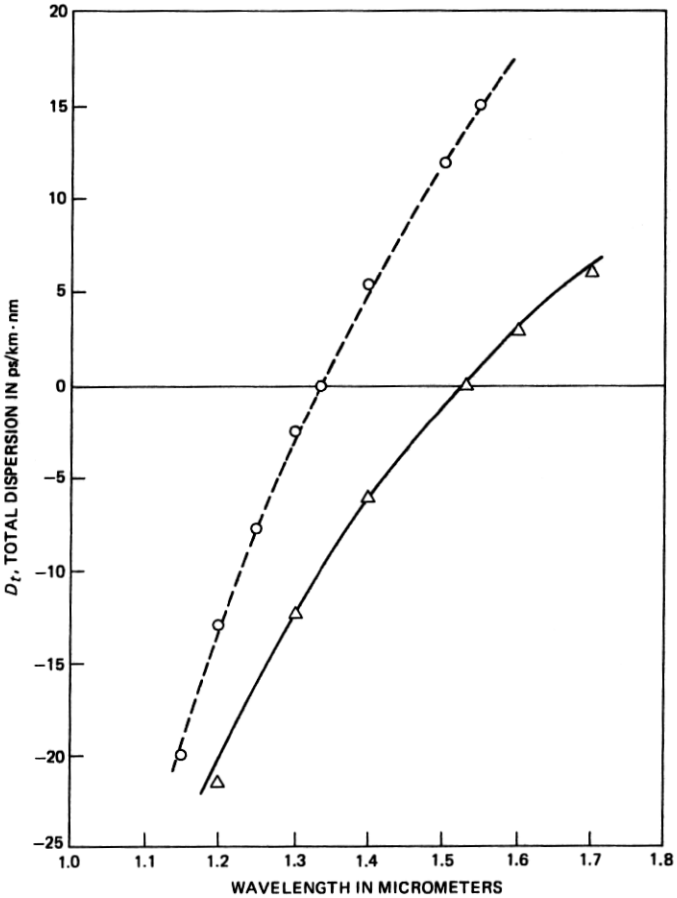

Fig. 8—A comparison of theory (dashed and solid lines) with experiment (see text).

$$\begin{vmatrix} 0 & (N_c^2/\kappa) - 1 & 0 & -MN_e/\kappa \\ \rho^2\kappa - M^2 & 0 & MN_e & 0 \\ 0 & MN_e/\kappa & 0 & \rho^2 - (M^2/\kappa) \\ -MN_e & 0 & N_e^2 - \kappa & 0 \end{vmatrix} . \quad (18)$$

The method of numerical computation has been given in our earlier work,[5] which briefly gives the procedure for finding the solutions and emphasizes what is needed to describe a single-mode fiber design.

Equation (17) is a familiar type of differential equation. A fourth-order Runge–Kutta method is used to solve it numerically. A concise description is as follows. First, we know that there are two possible solutions in both the core and cladding, and they are linearly independent. Therefore, a general solution will be a linear combination of

two solutions, denoted by Λ_i in the core and Γ_i in the cladding.

In the core region,

$$\Lambda_i = A_1\Lambda_{i1} + A_2\Lambda_{i2}, \tag{19}$$

and in the cladding region,

$$\Gamma_i = A_3\Lambda_{i3} + A_4\Lambda_{i4}. \tag{20}$$

The solutions Λ_{i1} and Λ_{i2} are transferred to the core-cladding interface through the operation of eq. (17), starting with two initial conditions given at the center of the core.[5,13]

At the interface $\rho = \rho_i$, each has to be matched with the solution in the cladding to satisfy the continuity condition mentioned earlier. Thus, the matching condition yields a set of homogeneous equations for the constants A_i. Hence, the characteristic equation is the vanishing determinant of the system of equations,

$$\det|\Lambda_{ij}| = 0. \tag{21}$$

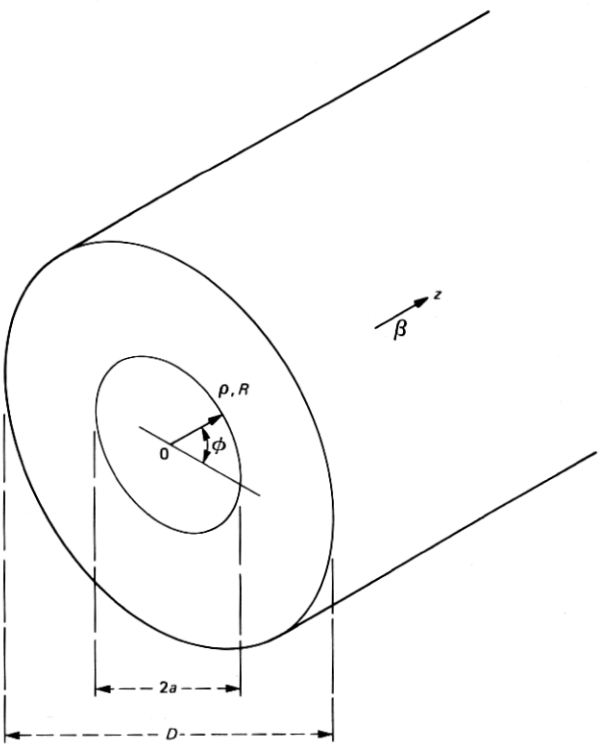

Fig. 9—Cross section of a fiber and cylindrical coordinate system. R or ρ is the radial coordinate, ϕ is the angle, and z is the axial direction ($\rho = KR$).

Particularly, considering $M = 0$, we can write the solutions in the core and cladding as follows. The two core solution vectors at $\rho = \rho_i$ are Λ_{i1} and $\Lambda_{i2}(\rho_i)$. Expressed in terms of their components, they are

$$\Lambda_{i1} = \begin{Bmatrix} \Lambda_{11} \\ \Lambda_{21} \\ \Lambda_{31} \\ \Lambda_{41} \end{Bmatrix} \quad \text{and} \quad \Lambda_{i2} = \begin{Bmatrix} \Lambda_{12} \\ \Lambda_{22} \\ \Lambda_{32} \\ \Lambda_{42} \end{Bmatrix}. \tag{22}$$

And the two cladding solutions at $\rho = \rho_i$ are taken as

$$\Lambda_{i3} = \begin{Bmatrix} \beta_1^2 \\ \kappa(\zeta_i)\gamma_0(\zeta_i) \\ 0 \\ 0 \end{Bmatrix} \cdot W_0(\zeta_i) \quad \text{and} \quad \Lambda_{i4} = \begin{Bmatrix} 0 \\ 0 \\ \gamma_0(\zeta_i) \\ \beta_1^2 \end{Bmatrix} \cdot W_0(\zeta_i), \tag{23}$$

where

$$\beta_1 = [N_e^2 - \kappa(\zeta_i)]^{1/2}, \qquad \zeta_i = \beta_i \rho_i,$$

$$\gamma_0 = \zeta_i \cdot [K_0'(\zeta_i)/K_0(\zeta_i)], \qquad \text{and} \qquad W_0(\zeta_i) = K_0(\zeta_i)/\beta_1^2.$$

The prime in the above equation denotes differentiation with respect to ζ.

REFERENCES

1. T. Miya, Y. Terunuma, T. Hosaka, and T. Miyashita, "Ultimate Low-Loss Single-Mode Fiber at 1.55 μm," Electron. Lett., *15* (1979), p. 106.
2. L. G. Cohen, C. Lin, and W. G. French, "Tailoring Zero Chromatic Dispersion Into the 1.5–1.6 μm Low-Loss Spectral Region of Single-Mode Fibers," Electron. Lett., *15* (1979), p. 334.
3. W. A. Gambling, H. Matsumura, and C. M. Ragdale, "Zero Total Dispersion in Graded-Index Single-Mode Fibers," Electron. Lett., *15* (1979), p. 474.
4. H. Tsuchiya and N. Imoto, "Dispersion-free Single-Mode Fiber in 1.5 μm Wavelength Region," Electron. Lett., *15* (1979), p. 476.
5. G. E. Peterson, A. Carnevale, U. C. Paek, and D. W. Berreman, "An Exact Numerical Solution to Maxwell's Equations for Lightguides," B.S.T.J., *59,* No. 7 (September 1980), pp. 1175–96.
6. G. E. Peterson, A. Carnevale, and U. C. Paek, "Comparison of Vector and Scalar Modes in a Lightguide with a Hyperbolic Secant Index Distribution," B.S.T.J., *59,* No. 9 (November 1980), pp. 1681–91.
7. J. W. Fleming, "Material Dispersion in Lightguide Glasses," Electron. Lett., *14* (1978), p. 326.
8. W. A. Gambling, D. N. Payne, and H. Matsumura, "Cut-Off Frequency in Radially Inhomogeneous Single-Mode Fiber," Electron. Lett., *13* (1977), p. 139.
9. Y. Kokubun and K. Iga, "Mode Analysis of Graded-Index Optical Fibers Using a Scalar Wave Equation Including Gradient-Index Terms and Direct Numerical Integration," J. Opt. Soc. Am., *70* (1980), p. 388.
10. T. Miya, Y. Terunuma, and T. Hosaka, "Fabrication of Single-Mode Fibers for 1.5 μm Wavelength Region," Dig. Jpn. Top. Meet., *OQE78-76* (1979).
11. D. Marcuse, "Microbending Losses of Single-Mode Step Index and Multimode, Parabolic-Index Fibers," B.S.T.J., *55,* No. 7 (September 1976), pp. 937–55.
12. V. J. Tekippe, "Evanescent Wave Coupling of Optical Fibers," presented at the Conference on the Physics of Fiber Optics at the 82nd Annual Meeting of the American Chemical Society, Chicago, Illinois, April 27–30, 1980.
13. M. O. Vassel, "Calculation of Propagating Modes in a Graded-Index Optical Fiber," Opto-Electron., *5* (1974), p. 271.
14. A. Vigants and S. P. Schlesinger, "Surface Waves On Radially Inhomogeneous Cylinders," IEEE Trans., *MTT-10* (1962), p. 375.